

Multi-energy, single-isotope imaging using stacked detectors

B.S. McDonald^{a,b,*}, S. Shokouhi^{b,c}, H.H. Barrett^d, T.E. Peterson^{a,b,c}

^aDepartment of Physics & Astronomy, Vanderbilt University, 1807 Station B Nashville, TN 37235, USA

^bInstitute of Imaging Science, Vanderbilt University, 1161 21st Avenue S., Nashville, TN 37232-2310, USA

^cDepartment of Radiology & Radiological Sciences, Vanderbilt University, 1161 21st Avenue S., Nashville, TN 37232-2675, USA

^dCollege of Optical Sciences and Department of Radiology, University of Arizona, 1630 E. University Blvd., Tucson, AZ 85721, USA

Available online 21 April 2007

Abstract

We investigated a scheme for concurrently detecting low- and high-energy emissions from ^{123}I with a stacked silicon double-sided strip detector (DSSD) and modular scintillation camera (Modcam) from the FastSPECT II design. We sequentially acquired both low- and high-energy emission images of an ^{123}I object with a prototype DSSD and a Modcam. A sandwich aperture increases spatial resolution in the low-magnification DSSD image via a smaller pinhole diameter and allows a higher magnification image on the Modcam. Molybdenum, the insert material, efficiently stops 20–30 keV photons due to its ~ 20 keV K-edge. Theoretically, less than 10% of 159 keV photons interact in 0.035 cm thick sheet of molybdenum, while this thickness stops virtually all ~ 30 keV photons. Thus, photons from both energy regions will be incident upon their respective detectors with little cross talk. With a multi-pinhole collimator, we can decode multiplexed images on the Modcam by making use of the lower-magnification DSSD image. This approach can provide an increase in system sensitivity compared to single-detector configurations. Using MCNP5 we examined the potential benefits and drawbacks of stacked detectors and the sandwich aperture for small-animal pinhole SPECT via the synthetic-collimator method. Simulation results encourage us to construct the novel aperture and use it with our new DSSDs designed for mounting in a transmission configuration.

© 2007 Elsevier B.V. All rights reserved.

PACS: 87.58.Ce

Keywords: Pinhole collimator; ^{123}I ; Small-animal imaging; Monte Carlo; SPECT

1. Introduction

Advances in *in vivo* imaging instrumentation allow researchers to study animal models of disease and drug response with greater clarity. Detectors with high spatial resolution coupled with multi-pinhole collimators allow for high sensitivity and resolution in small-animal nuclear imaging. With silicon double-sided strip detectors (DSSDs), we can image low-energy X-ray or gamma-ray emissions from radioisotopes such as ^{125}I and ^{123}I quite well. Prior work with DSSDs [1] has shown that stacking DSSDs improves total efficiency with minimal image degradation due to cross-detector scattering.

Certain isotopes emit similar amounts of low- and high-energy photons. For instance, ^{123}I emits near equal amounts of 27–31 keV X-rays and 159 keV gamma-rays. Usually, just one energy regime is used for imaging. By stacking a modular scintillation camera (Modcam) from the FastSPECT II design [2] behind a DSSD, it is possible to utilize more of the radioisotope emissions for imaging.

2. Basic measurements

We made sequential acquisitions with a prototype DSSD and a Modcam. A sample image and line profile are shown in Fig. 1. Two capillaries of 1.1 mm inner diameter were filled with $\sim 550 \mu\text{Ci}$ of Na ^{123}I solution and placed 3.5 mm apart in an acrylic holder. A single 500 μm diameter gold pinhole insert in a tungsten alloy collimator plate was used to make both images, with the location of the sources relative to the pinhole kept the same for both acquisitions.

*Corresponding author. Department of Physics & Astronomy, Vanderbilt University, 1807 Station B, Nashville, TN 37235, USA.

E-mail address: ben.mcdonald@vanderbilt.edu (B.S. McDonald).

Count time was 10 min for each image. Magnifications were $0.9\times$ for the DSSD image and $2\times$ for the Modcam image.

These results show that imaging the different energy emissions from ^{123}I is possible sequentially with a DSSD and a Modcam.

3. Sandwich aperture

We can better utilize the high intrinsic spatial resolution of the DSSD with smaller pinholes and a novel aperture. The sandwich aperture consists of two tungsten plates with a 1.0 mm diameter pinhole enveloping a molybdenum plate with a nested, 300 μm diameter pinhole. Fig. 2 shows the geometry for two keel-edge pinholes.

Constructing such a device requires precise machining of tungsten alloys and micro-pinholes. Sheets of molybdenum are readily available in different thicknesses. For micro-pinholes, electron discharge machining and tomo lithographic molding (Mikro Systems, Inc., Charlottesville, VA) are the most accurate methods.

4. Monte Carlo modeling

An obvious concern with stacked detectors is that the higher energy gammas will interact in the DSSD or the insert before depositing energy in the Modcam, blurring the resulting images. With MCNP5 [3], we examined the amount of detector scatter, collimator scatter, collimator penetration, and high-energy down-scatter to determine the feasibility of stacked detectors and the sandwich aperture for a novel imaging method.

4.1. Simulation details

The simulation geometry included two stacked detectors. A $6.0\times 6.0\times 0.1\text{ cm}^3$ DSSD and a $10.0\times 10.0\times 0.5\text{ cm}^3$ NaI(Tl) crystal were modeled along with a dual-aperture pinhole collimator. Quartz lightguide material was modeled and photomultiplier tubes were approximated as 20% density silicon dioxide. The full opening angle of both pinholes was 60° . The full ^{123}I spectrum was incorporated and 50 million photons were confined to emit within a cone with a 24.5° half-angle. The point source was placed 4 cm

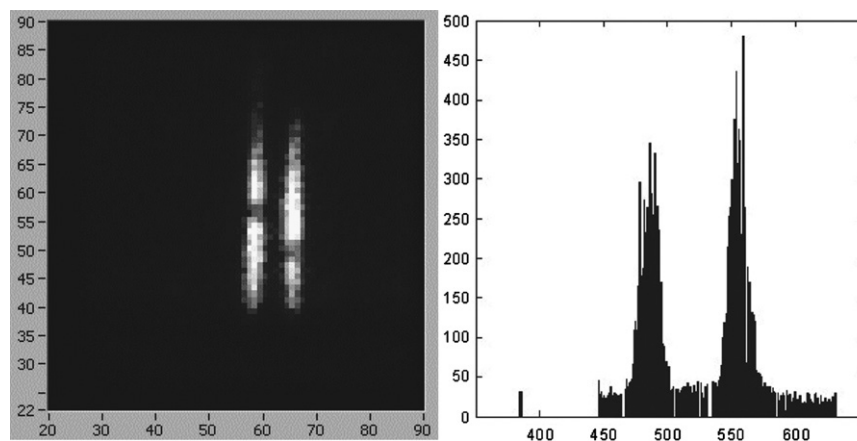


Fig. 1. Modcam image of the two line sources (left). Axes are in millimeters. The right figure shows a line profile through the prototype DSSD image (counts vs. strip number (50 μm strip pitch)). At $2\times$ and $0.9\times$ magnifications, line projections are $\sim 7\text{ mm}$ (A) and $\sim 3.2\text{ mm}$ (B) apart.

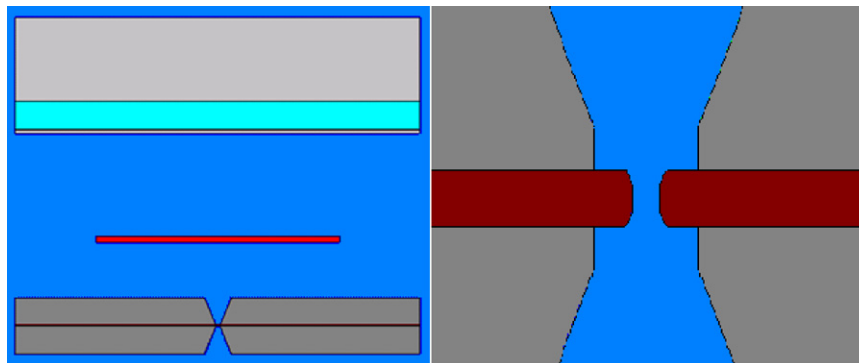


Fig. 2. The inset in the right figure is a 0.035 cm thick, 0.03 cm diameter molybdenum pinhole, whereas the larger pinhole is a 1.0 cm thick tungsten collimator with a 0.1 cm pinhole diameter. The image on the right is a magnified section of the bottom middle region of the figure on the left. The thin central object is the 1.0 mm thick DSSD and upper objects are the Modcam components.

from the pinhole plane so that the conical part of the tungsten pinhole was fully illuminated during both on- and off-axis simulations. Detectors were placed 1.0 cm (DSSD) and 4.0 cm (Modcam) from the pinhole plane. Collimator penetration and scatter are significant near the edges of any pinhole, so keel-edge pinholes were modeled as they help mitigate these effects. The channel heights of the tungsten and molybdenum pinholes were 0.087 and 0.22 cm, respectively. Four simulations were run of the permutations of on- and off-axis source and with and without the DSSD and sandwich aperture.

We accounted for the Modcam's spatial resolution by convolving the profiles with a 2.0 mm full-width at half-maximum (FWHM) Gaussian filter. The energy windows for the Modcam and the DSSD were 15% at 159 keV and 22% at 27 keV, respectively.

4.2. Simulation results

Ignoring scatter in the collimator, 1.6% of photons in the Modcam window scatter in the DSSD before depositing their energy in the scintillator. Conversely, 1.3% of detected events in the DSSD first scatter in the Modcam.

Fig. 3 shows that with a 0.030 cm thick molybdenum insert and the DSSD, the line profile through the projection on the Modcam is peaked due to the 300 μm pinhole. The off-axis profiles are roughly 1 mm narrower (FWHM) than the on-axis profiles due to occlusion by the keel-edge pinhole. The DSSD and pinhole insert decrease the Modcam sensitivity by 5.1% on-axis and by 8.6% off-axis, but no appreciable change in the widths of the distributions was observed.

The amounts of collimator scatter and penetration in the detected events for each detector are given in Table 1. We followed the tack of others [4–6] for this aspect. Penetra-

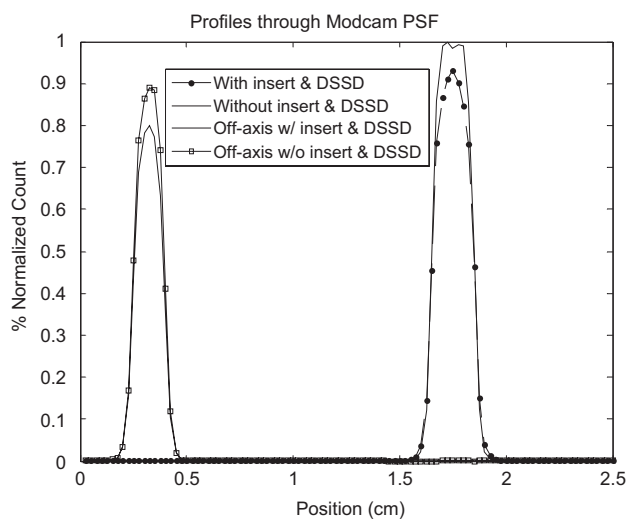


Fig. 3. Line profiles through on- (right) and 20° off-pin-hole-axis point spread functions on the Modcam with and without the molybdenum insert and the DSSD. Counts were normalized to the peak count of the simulation without the insert and DSSD.

Table 1

Photon primary, penetration and scatter components for on-pin-hole-axis source with the sandwich aperture

Events (%)	Direct (%)	Penetration (%)	Scatter in Mo (%)	Scatter in W (%)
DSSD	74.6	22.3	1.0	2.1
Modcam	84.4	12.4	1.0	2.2

tion includes photons that pass through either collimator material, and scattering includes both coherent (Rayleigh) and Compton interactions.

5. Discussion

Detecting the X-ray emissions that are normally ignored with our scheme suggests a system improvement in sensitivity over standard pinhole apertures with single detectors. Without the sandwich aperture, 54% more incident photons are detected by including the DSSD. Adding the sandwich aperture reduces the 54% increase to 6%. The number of 159 keV photons incident on the Modcam is decreased by 5–9% due to the DSSD and insert, as shown in Fig. 3. Therefore, sensitivity gains from the DSSD are nearly overcome by cross-detector scatter and attenuation in the sandwich aperture. A larger molybdenum aperture (e.g. 500 μm diameter), in a multi-pin-hole configuration would enable a net gain in sensitivity.

Results from the line profiles indicate that we should consider using a thinner molybdenum insert so the 159 keV photons are less attenuated, and hence the profile in Fig. 3 with the insert and DSSD less peaked. However, as the insert is made thinner, fewer low-energy photons are stopped. An optimal thickness must be derived.

The high amount of collimator penetration in the DSSD reported in Table 1 is nearly all from 159 keV photons that deposit only part of their energy via Compton scattering. Low-energy photon penetration amounts to less than 1% of events in the DSSD energy window. This means that we will effectively be imaging at two pinhole diameters on the DSSD, for low-energy photons and for high-energy photons that Compton scatter in the detector. Again, by increasing the size of the inner molybdenum pinhole, we can decrease the penetrative component.

Our scheme constitutes a particular implementation of the physical part of the ‘synthetic-collimator’ method [7]. The synthetic-collimator consists of a multi-pin-hole aperture, a high-resolution detector, and an algorithm for estimating the radiotracer distribution for a measured data set. Each pinhole defines a projection direction and reasonable limited-angle reconstructions can be obtained with our geometry and compact objects. The pinholes must provide adequate angular sampling of the object and images must be acquired at multiple detector–pinhole distances. With a multi-pin-hole collimator, low-magnification images occupy a smaller area on the DSSD and

projections thus have less overlap for a given number of pinholes. We can use many pinholes without multiplexing on the DSSD. These data give information about multiplexing of the more magnified projections on the Modcam for multi-pinhole imaging and help produce artifact-free SPECT reconstructions. Furthermore, a stacked detector scheme removes the need for a motion system for collecting the different detector–pinhole distance projections required for synthetic-collimator reconstruction. Eliminating or widening the molybdenum pinhole and merely adjusting the detector–pinhole distance may be more effective for synthetic-collimator studies. How extra resolution in the DSSD image affects the synthetic-collimator reconstructions will determine the fate of the sandwich aperture. Overall, simulations indicate that the interdetector cross talk should be of a level that the stacked detector, dual-energy imaging method is worth continued investigation.

5.1. Future directions

We plan to build various pinhole apertures and use them with our new DSSDs, which are designed specifically for mounting in a stacked format. We also will develop a shielded container that allows multiple stacked detector scenarios. Sets of stacked detectors placed orthogonally to each other will increase the projection views and likely

improve synthetic-collimator results. We plan to explore other regions of the collimator parameter space and determine optimal detector configurations for the synthetic collimator.

Acknowledgments

This work was supported by NIH Grants R33 EB000776-04 and P41 EB002035-07. The research of Todd E. Peterson, Ph.D. is supported in part by a Career Award at the Scientific Interface from the Burroughs Wellcome Fund.

References

- [1] T.E. Peterson, D.W. Wilson, H.H. Barrett, IEEE Nucl. Sci. Symp. Conf. Record (2003) 1984.
- [2] L.R. Furenlid, D.W. Wilson, et al., IEEE Trans. Nucl. Sci. NS-51 (3) (2004) 631.
- [3] MCNP—A General Monte Carlo N-Particle Transport code—version 5.1.14, Los Alamos National Laboratory (URL: <http://mcnp-green.lanl.gov/index.html>).
- [4] H.M. Deloar, et al., Phys. Med. Biol. 48 (2004) 995.
- [5] F. Van der Have, F.J. Beekman, Phys. Med. Biol. 49 (2004) 1369.
- [6] D.N. Jangha, R.A. Mintzer, J.D. Valentine, J.N. Aarsvold, IEEE Nucl. Sci. Symp. Conf. Record (2001) 1309.
- [7] D.W. Wilson, H.H. Barrett, E.W. Clarkson, IEEE Trans. Med. Imaging 19 (2000) 412.